

GRADIENT OF THE DISCRETIZED ENERGY METHOD AND DISCRETIZED CONTINUOUS GRADIENT IN ELECTROMAGNETIC SHAPING SIMULATION

JEAN R. ROCHE*

The goal of this paper is to study the differences between two approaches to gradient computation in shape optimization. Simulation methods in shape optimization require computation of a local minimum of an energy function by descent methods, which involves the gradient computation with respect to shape perturbations. Two different approaches are mainly used in optimal shape computations. The first one consists in computing a zero of a continuous gradient approximation. The second one consists in computing a zero of the shape derivative of a discretized version of the cost function. In this paper, we study the differences between the two approaches in electromagnetic shaping simulation.

1. Introduction

In (Henrot and Pierre, 1989) the authors consider an electromagnetic casting problem in the two-dimensional case. The optimal shape is characterized as a local minimum of an energy functional depending on the shape and the solution of the partial differential equation. In (Novruzi and Roche, 1995; Pierre and Roche, 1991; 1993) we have introduced a numerical shape optimization approach where we have computed a critical point by numerical minimization of the cost function. We seek for an approximate solution in a set of domains with piecewise linear boundary. This procedure transforms the continuous problem into a finite-dimensional problem, where the optimization parameters are the nodes of the piecewise linear boundary representation. Any classical numerical descent optimization technique necessitates the computation of a good approximation of the shape gradient. Here two techniques can be used. The first one, called the GCD method, consists in computing a continuous shape derivative and then evaluating a numerical approximation. The second one, called the GD method, consists in computing the gradient of the numerical approximation of the goal function. In (Novruzi and Roche, 1995; Pierre and Roche, 1991; 1993) we have applied the first technique. In the present paper, we set up a purely discrete problem and then we compare the two methods.

The relation between these two methods has been studied by Chenais (1992), Lods (1992) and Masmoudi (1987) with the shape-optimization problem considered

* CNRS UMR 9973 & INRIA-Lorraine (Projet NUMATH), Laboratoire de Mathématiques, Université de Nancy I (UHP), BP 239, 54506 Vandoeuvre-lès-Nancy Cedex, France, e-mail: roche@iecn.u-nancy.fr.

as a control problem. The conclusion is that the discretization of the continuous gradient and the gradient of the discrete cost function are the same if we use an interior approximation of the geometry and the solution of the elliptic problem. This is not our case and we study the numerical difference in the results and the computational complexity.

2. Variational Formulation

2.1. Problem Statement

The simplified model of the electromagnetic shaping problem studied here concerns the case of a vertical column of liquid metal falling down into an electromagnetic field created by vertical conductors. We assume that the frequency of the imposed current is very high so that the magnetic field does not penetrate into the metal. In other words, we neglect the skin effect. The electromagnetic forces are reduced to the magnetic pressure acting on the interface.

We denote by ω an open and bounded domain of class C^2 in \mathbb{R}^2 and by Ω the complement of $\bar{\omega}$. Let Γ be the boundary of ω , and denote by ν_i and ν_e the inward and outward normals to Γ , respectively. Under suitable assumptions (Henrot and Pierre, 1989; Novruzi and Roche, 1995; Pierre and Roche, 1991; 1993), the equilibrium configurations are given by a local critical point of the following total energy:

$$E(\omega, \varphi) = \frac{-1}{2\mu_0} \int_{\Omega} |\nabla\varphi|^2 dx + \sigma P(\omega) \quad (1)$$

where $P(\omega)$ is the perimeter of ω (i.e. the length of Γ when Γ is regular enough, for instance of class C^1)

$$P(\omega) = \int_{\Gamma} d\Gamma \quad (2)$$

$d\Gamma$ being the length measure of Γ .

In (1) σ is the surface tension of the liquid and φ is the solution of the problem:

$$-\Delta\varphi(x) = \mu_0 \bar{j}_0(x) \quad \text{in } \Omega \quad (3)$$

$$\varphi(x) = 0 \quad \text{on } \Gamma \quad (4)$$

$$|\varphi(x)| = O(1) \quad \text{as } |x| \rightarrow \infty \quad (5)$$

$$|\nabla\varphi(x)| = O(|x|^{-1}) \quad \text{as } |x| \rightarrow \infty \quad (6)$$

where $\bar{j}_0 = (0, 0, j_0)$ stands for the density current vector and μ_0 is the vacuum permeability. The support of j_0 is in the interior of Ω .

Lemma 1. *The exterior Dirichlet problem (3)–(6) has a unique solution in $W_0^1(\Omega)$.*

Proof. See (Kress, 1982). ■

If we introduce the function:

$$u(x) = \frac{-\mu_0}{2\pi} \int_{\mathbb{R}^2} \ln|x-y|j_0(x) dy + \frac{\mu_0}{2\pi} \ln|x| \int_{\mathbb{R}^2} j_0(y) dy \tag{7}$$

which satisfies

$$-\Delta u = \mu_0 j_0 \quad \text{in } \mathbb{R}^2 \tag{8}$$

$$|u| = O(|x|^{-1}) \quad \text{as } |x| \rightarrow \infty \tag{9}$$

$$|\nabla u| = O(|x|^{-2}) \quad \text{as } |x| \rightarrow \infty \tag{10}$$

then the problem (3)–(6) is equivalent to:

$$\varphi(x) = u(x) + v(x) \quad \text{in } \bar{\Omega}$$

where

$$-\Delta v(x) = 0 \quad \text{in } \Omega \tag{11}$$

$$v(x) = -u(x) \quad \text{on } \Gamma \tag{12}$$

$$|v(x)| = O(1) \quad \text{as } |x| \rightarrow \infty \tag{13}$$

Remark 1. Using Green’s formula and the boundary conditions on Γ (4) and (12) we have

$$\int_{\Omega} (|\nabla\varphi|)^2 dx = - \int_{\Gamma} u(x) \frac{\partial\varphi(x)}{\partial\nu_e} d\Gamma - \mu_0 \int_{\text{supp}(j_0)} u(x)j_0(x) dx \tag{14}$$

where $\text{supp}(j_0) = \{x : j_0(x) \neq 0\}$. Then we can give a representation of the energy useful for numerical calculations:

$$E(\omega, \varphi) = \frac{1}{2\mu_0} \int_{\Gamma} u(x) \frac{\partial\varphi(x)}{\partial\nu_e} d\Gamma + \frac{1}{2} \int_{\text{supp}(j_0)} u(x)j_0(x) dx + \sigma \int_{\Gamma} d\Gamma \tag{15}$$

or

$$E(\omega, \varphi) = \frac{-1}{2\mu_0} \int_{\Gamma} u(x) \frac{\partial\varphi(x)}{\partial\nu_i} d\Gamma + \frac{1}{2} \int_{\text{supp}(j_0)} u(x)j_0(x) dx + \sigma \int_{\Gamma} d\Gamma \tag{16}$$

Remark 2. This problem or very similar ones have been considered by several authors. We refer the reader to the following papers and to references therein for physical analysis of the simplifying assumptions that the above model requires: see Brancher *et al.* (1983), Brancher and Sero-Guillaume (1983), Coulaud and Henrot (1994), Etay (1982), Gagnoud *et al.* (1986), Mestel (1982), Sero-Guillaume (1983), Shercliff (1981), Sneyd and Moffatt (1982).

The variational formulation of (1)–(6) consists in considering the equilibrium domain ω as a stationary point for the total energy (1), under the constraint that the measure of ω is given by S_0 .

In (Henrot and Pierre, 1989; Pierre and Roche, 1991) it is shown that the equilibrium relation is given on the boundary of ω by

$$\frac{1}{2\mu_0}|\nabla\varphi|^2 + \sigma\mathcal{H} = \Lambda \quad \text{on } \Gamma \tag{17}$$

where \mathcal{H} is the curvature of Γ (seen from the metal), σ is the surface tension of the liquid and $|\cdot|$ denotes the euclidean norm. The constant Λ is an unknown of the problem, and so is the boundary Γ .

To establish the equilibrium relation (17), we consider the following Lagrangian operator:

$$L(\omega, \varphi, \Lambda) = E(\omega, \varphi) + \Lambda \left(\text{meas}(\omega) - S_0 \right) \tag{18}$$

In the next subsection, we introduce a framework to compute first shape derivatives of L and establish necessary conditions.

2.2. Derivation

In order to introduce shape optimization techniques, we consider shape derivatives. We can distinguish a few approaches to derivation with respect to the shape in (Sokolowski and Zolesio, 1992).

Let V be a regular vector field (e.g. $C^1(\mathbb{R}^2, \mathbb{R}^2)$) with compact support in an open neighborhood of Ω , and ν be the outward normal to ω . We consider domain deformations defined by the mapping:

$$T_t(V) : x \rightarrow x + tV(x) \tag{19}$$

and we set $\Omega_t = T_t(V)(\Omega)$.

Next we denote by φ_t the solution to the exterior Dirichlet problem (3)–(6) when we replace Ω by Ω_t . Then the shape derivative of φ is given by

$$\varphi'(x) = \lim_{t \rightarrow 0} \frac{\varphi_t(x) - \varphi(x)}{t} \tag{20}$$

This derivative exists if Ω has a Lipschitz boundary. The shape derivative of φ is the solution of the following elliptic exterior problem (Simon, 1980):

$$\begin{aligned} -\Delta\varphi'(x) &= 0 && \text{in } \Omega \\ \varphi'(x) &= -V(x) \cdot \nabla\varphi(x) && \text{on } \Gamma \\ |\varphi'(x)| &= O(1) && \text{as } |x| \rightarrow \infty \end{aligned} \tag{21}$$

Given an integral operator $E(\omega, \varphi)$ which depends on the shape ω and on the solution φ of the boundary-value problem, we can define

$$\frac{d}{dt}E(\omega_t, \varphi_t) \Big|_{t=0} = \lim_{t \rightarrow 0} \frac{E(\omega_t, \varphi_t) - E(\omega, \varphi)}{t} \tag{22}$$

Then we can compute the shape derivatives of operators depending on ω , Γ and φ .

If

$$G_1(\omega_t, \varphi_t) = \int_{\omega_t} g(\omega_t, \varphi_t) \, dx \tag{23}$$

then

$$\frac{d}{dt} G_1(\omega_t, \varphi_t) \Big|_{t=0} = \int_{\omega} \frac{d}{dt} g(\omega_t, \varphi_t) \Big|_{t=0} \, dx + \int_{\Gamma} g(\omega, \varphi) V \cdot \nu_e \, d\Gamma \tag{24}$$

and if

$$G_2(\omega_t, \varphi_t) = \int_{\Gamma_t} g_2(\Gamma_t, \varphi_t) \, d\Gamma \tag{25}$$

then we have

$$\frac{d}{dt} G_2(\omega_t, \varphi_t) \Big|_{t=0} = \int_{\Gamma} \frac{d}{dt} g_2(\Gamma_t, \varphi_t) \Big|_{t=0} \, d\Gamma + \int_{\Gamma} g_2(\Gamma, \varphi) \mathcal{H} V \cdot \nu_e \, d\Gamma \tag{26}$$

where \mathcal{H} is the curvature of Γ .

Using the framework just introduced we have the following Lemma.

Lemma 2. *If $V \in C^1(\mathbb{R}^2, \mathbb{R}^2)$ with support in an open neighborhood of ω , Γ is of class C^2 , and L is defined by (18), then we have*

$$\frac{d}{dt} L(\omega_t, \varphi_t, \Lambda)(V) \Big|_{t=0} = \frac{1}{2\mu_0} \int_{\Gamma} \left\{ \left(\frac{\partial \varphi}{\partial \nu_e} \right)^2 + \sigma \mathcal{H} + \Lambda \right\} V \cdot \nu_e \, d\Gamma \tag{27}$$

or

$$\begin{aligned} \frac{d}{dt} L(\omega_t, \varphi_t, \Lambda)(V) \Big|_{t=0} &= \frac{1}{2\mu_0} \int_{\Gamma} \left\{ u \frac{\partial \varphi'}{\partial \nu_e} + \frac{\partial}{\partial \nu_e} u(x) \frac{\partial \varphi}{\partial \nu_e}(x) \right. \\ &\quad \left. - \mathcal{H} u(x) \frac{\partial \varphi(x)}{\partial \nu_e} \right\} V \cdot \nu_e \, d\Gamma \\ &\quad + \int_{\Gamma} (\sigma \mathcal{H} + \Lambda) V \cdot \nu_e \, d\Gamma \end{aligned} \tag{28}$$

where \mathcal{H} is the curvature of Γ seen from ω .

Proof. If $E(\omega, \varphi)$ is given by (1), then

$$\begin{aligned} \frac{d}{dt} L(\omega_t, \varphi_t, \Lambda) \Big|_{t=0} (V) &= \frac{-1}{2\mu_0} \left(\int_{\Gamma} 2\nabla \varphi \nabla \varphi' \, dx - \int_{\Gamma} (\nabla \varphi)^2 V \cdot \nu_e \, d\Gamma \right) \\ &\quad + \sigma \int_{\Gamma} \mathcal{H} V \cdot \nu_e \, d\Gamma + \Lambda \int_{\Gamma} V \cdot \nu_e \, d\Gamma \end{aligned}$$

But

$$\int_{\Omega} \nabla\varphi \nabla\varphi' = \int_{\Gamma} \varphi \frac{\partial\varphi'}{\partial\nu_e} d\Gamma - \int_{\Omega} \varphi \Delta\varphi' dx = 0 + 0$$

since φ' is the solution of (21), and $\varphi = 0$ to Γ by (4).

If $E(\omega, \varphi)$ is given by (15), using (26) and the fact that $u' \equiv 0$, we obtain the second representation of the shape derivative of the Lagrangian L . ■

Remark 3. The expression (27) is true only in the case of a regular boundary Γ . In the case of a boundary which is only piecewise linear, the problem is radically different. The first derivative of the energy term involving the magnetic field may not exist at all. For the perimeter term we can give an expression for the first derivative even in the case of a piecewise linear boundary, see (Sokolowski and Zolesio, 1992).

Remark 4. The equilibrium relation (17) implies the first-order necessary condition:

$$\frac{d}{dt} L(\omega_t, \varphi_t, \Lambda) \Big|_{t=0} (V) = 0 \quad \text{for all } V \in C^1(\mathbb{R}^2, \mathbb{R}^2) \tag{29}$$

3. Discretized Approach

3.1. Discretized Problem

We construct numerically a minimizing sequence of domains ω^k . More precisely, we consider a sequence of domains determined by their boundaries $\partial\omega^k$. In the sequel, $\Gamma^k = \partial\omega^k$ stands for a piecewise linear Jordan curve with edges $\ell_i = [z_i^k, z_{i+1}^k]$, $i = 1, \dots, n$ and $z_{n+1}^k = z_1^k$. We introduce a parametric representation of each ℓ_i :

$$\bar{x}_i(t) = (1 - t)\bar{z}_i^k + t\bar{z}_{i+1}^k = \left(x_i^1(t), x_i^2(t)\right)^t \tag{30}$$

Let $L_i = ((\dot{x}_i^1)^2 + (\dot{x}_i^2)^2)^{1/2} = \|z_{i+1} - z_i\|$ be the length of the segment $[z_i, z_{i+1}]$ and $h = \max\{L_i, i = 1, \dots, n\}$.

At each iteration of the minimizing algorithm, the boundary Γ^{k+1} is obtained by a local perturbation of Γ^k . To each vertex z_i^k of Γ^k is associated a direction $\hat{Z}_i^k \in \mathbb{R}^2$. We construct a continuous piecewise linear function $Z_i^k : \Gamma^k \rightarrow \mathbb{R}^2$ such that

$$Z_i^k(z_j^k) = \hat{Z}_i^k \delta_{ij}, \quad i, j = 1, \dots, n \tag{31}$$

Then the perturbation vector field defined on Γ^k is given by $Z^k(x) = \sum_{i=1}^n \xi_i Z_i^k(x)$ and the new surface Γ^{k+1} is constructed from Γ^k by

$$\Gamma^{k+1} = \left\{ X = x + \sum_{i=1}^n \xi_i Z_i^k(x) = \left(I + \sum_{i=1}^n \xi_i Z_i^k\right)(x); \xi_i \in \mathbb{R}; x \in \Gamma^k \right\} \tag{32}$$

where $\bar{\xi}^t = (\xi_1, \dots, \xi_n)$ are the unknowns which determine the evolution of the surface Γ^k . In practice, the continuous minimization problem reduces to an n -dimensional optimization problem depending on the solution of the exterior Dirichlet problem (11)–(13).

For numerical purposes, we consider the following penalized energy:

$$E_r(\omega^k, \varphi^k) = E(\omega^k, \varphi^k) + \frac{r}{2} \left(\text{meas}(\omega^k) - S_0 \right)^2 \tag{33}$$

Then, using the notation just introduced, the penalized energy (33) has the following form:

$$\begin{aligned} E_r(\omega^k, \varphi^k) = & \frac{1}{2\mu_0} \sum_{i=1}^n \left(\int_0^1 u(x_i(t)) \frac{\partial \varphi^k}{\partial \nu_e}(x_i(t)) L_i dt + \sigma L_i \right) \\ & + \frac{r}{2} \left(\sum_{i=1}^n \int_0^1 \dot{x}_i^2(t) x_i^1(t) L_i dt - S_0 \right)^2 + \int_{\Omega} u(x) j_0 dx \end{aligned} \tag{34}$$

or

$$\begin{aligned} E_r(\omega^k, \varphi^k) = & \frac{-1}{2\mu_0} \int_{\Omega^k} (\nabla \varphi^k \nu_e)^2 dx + \sigma \sum_{i=1}^n L_i \\ & + \frac{r}{2} \left(\sum_{i=1}^n \int_0^1 \dot{x}_i^2(t) x_i^1(t) L_i dt - S_0 \right)^2 \end{aligned} \tag{35}$$

The expression (34) is useful in numerical calculations because we suppose that we know the value of the expression:

$$\int_{\Omega^k} u(x) j_0(x) dx = \int_{\text{supp}(j_0)} u(x) j_0(x) dx \tag{36}$$

which is independent of ω .

Remark 5. For a piecewise linear approximation of Γ we know that the error between $x \in \Gamma^k$ and its projection on Γ is of order h^2 , where h is the maximum length of the l_i segments (Nedelec, 1977).

3.2. Exterior Dirichlet Problem

At each iteration, we have to solve the following exterior problem:

$$-\Delta v(x) = 0 \quad \text{in } \Omega^k \tag{37}$$

$$v(x) = -u(x) \quad \text{on } \partial\omega^k = \Gamma^k \tag{38}$$

$$|v(x)| = O(1) \quad \text{as } |x| \rightarrow \infty \tag{39}$$

Following Kress (1982), an integral single layer representation of the solution to (37)–(39) is given by

$$v(x) = \frac{-1}{2\pi} \int_{\Gamma^k} q(y) \ln |x - y| d\Gamma + c \tag{40}$$

with $q(y) \in H^{-1/2}(\Gamma^k)$ and

$$\int_{\Gamma^k} q(y) d\Gamma = 0 \tag{41}$$

The constant c is the value of v at the infinity. Then

$$\frac{\partial v}{\partial \nu_x}(x) = \frac{-1}{2\pi} \int_{\Gamma^k} q(y) \frac{\partial \ln |x - y|}{\partial \nu_x} d\Gamma + \frac{1}{2}q(x) \quad \text{if } x \in \Gamma \tag{42}$$

Here the unknown is the density $q(y)$ and we compute it using the boundary condition (38) in a weak formulation. We seek $q(y) \in H^{-1/2}(\Gamma^k)$ as a solution of the following problem:

$$\frac{-1}{2\pi} \int_{\Gamma^k} g(x) \int_{\Gamma^k} q(y) \ln |x - y| d\Gamma d\Gamma + c \int_{\Gamma^k} g(x) d\Gamma = - \int_{\Gamma^k} u(x)g(x) d\Gamma \tag{43}$$

and

$$\int_{\Gamma^k} q(x) d\Gamma = 0 \tag{44}$$

for all $g \in H^{-1/2}(\Gamma)$.

In numerical calculations, we consider a piecewise constant approximation $q_h(x)$ of $q(x)$:

$$q_h(x) = \sum_{i=1}^n q_i e_i(x) \tag{45}$$

where $e_i(x) = 1$ if $x \in [z_i, z_{i+1}]$ and zero elsewhere.

Then we obtain a linear system:

$$A\bar{q} = b \tag{46}$$

where

$$a_{i,j} = \frac{-1}{2\pi} \int_{\ell_i} \int_{\ell_j} \ln |x - y| d\Gamma d\Gamma, \quad i, j = 1, \dots, n \tag{47}$$

$$a_{i,j} = \int_{\ell_j} d\Gamma, \quad j = 1, n \text{ and } i = n + 1 \tag{48}$$

$$a_{i,j} = a_{j,i} \tag{49}$$

$$a_{n+1,n+1} = 0 \tag{50}$$

$$(\bar{q})_j = q_j, \quad j = 1, \dots, n \tag{51}$$

$$q_{n+1} = c \tag{52}$$

$$b_i = - \int_{\ell_i} u(x) \, d\Gamma, \quad i = 1, n \tag{53}$$

Remark 6. The linear system (46) is symmetric and dense, so we use a LDL^t decomposition of A . The numerical approximation of the normal derivative in (42) is computed by a Gauss quadrature.

Remark 7. If q is the solution of the system (43),(44) and \bar{q} is the solution of (46) with piecewise constant approximation, we have the following error boundary (Nedelec, 1977):

$$\|q - \bar{q}\|_{H^{-1/2}(\Gamma)} \leq C_1 h \|q\|_{H^1(\Gamma)} \tag{54}$$

and

$$\left\| \frac{\partial v}{\partial \nu} - \frac{\partial \bar{v}^k}{\partial \nu} \right\|_{H^{-1/2}(\Gamma)} \leq C_2 h \|q\|_{H^1(\Gamma)} \tag{55}$$

Remark 8. The numerical computation of the coefficients $a_{i,j}$, $i, j = 1, \dots, n$ requires $l \times n^2$ floating-point operations (flops). The integer l is the product of $K \times K$ and the number of flops needed to compute a logarithm, where K is the number of numerical-quadrature nodes. Computing the L^tDL decomposition of the matrix A requires $n^3/6$ flops. Once the L^tDL is known, the computation of q_i , $i = 1, \dots, n$ needs $n^2 + n$ flops. Thus the computation of \bar{q} demands $(n^3/6) + (l + 1) \times n^2 + n$ flops.

Remark 9. The approximation of the normal derivative of $\partial v / \partial \nu_e$ at $x_l \in \ell_l$ is given by

$$\frac{\partial \bar{v}^k}{\partial \nu_e}(x_l) = \frac{-1}{2\pi} \sum_{\substack{i=1 \\ i \neq l}}^n q_i \sum_{m=1}^K p_m \frac{\partial \ln |x_l - x_i(s_m)|}{\partial \nu_e} + \frac{1}{2} q_l \tag{56}$$

Accordingly, the computation of $\partial \bar{v}^k(x_l) / \partial \nu_l$ requires $O(n)$ floating-point operations.

3.3. Discretized Continuous Gradient

Using the shape-derivation techniques introduced in Section 2, we obtain the continuous gradient of the penalized energy (33).

Lemma 3. *If $V \in C^1(\mathbb{R}^2, \mathbb{R}^2)$ with support in an open neighborhood of ω , $\Gamma \in C^2$ and E_r is defined by (33), we have then:*

$$\begin{aligned} \frac{d}{dt} E_r(\omega_t, \varphi_t)(V) \Big|_{t=0} &= \frac{1}{2\mu_0} \int_{\Gamma} \left(\left(\frac{\partial \varphi}{\partial \nu_e} \right)^2 + \sigma \mathcal{H} \right) V \cdot \nu_e \, d\Gamma \\ &+ r \left(\text{meas}(\omega) - S_0 \right) \int_{\Gamma} V \cdot \nu_e \, d\Gamma \end{aligned} \tag{57}$$

where \mathcal{H} is the curvature of Γ seen from ω .

Proof. This result may be proved in much the same way as Lemma 2. ■

The discretized continuous gradient (GCD, “Gradient Continu Discretisé” in French) is a numerical approximation of (57) using the framework introduced in Section 3.1. To compute the boundary integrals, we used an interior Gauss-Legendre quadrature method with integration points $x_i(s_m)$, $i = 1, \dots, n$ and $m = 1, \dots, K$. We denote by p_m the associated weights.

Then for $i = 1, \dots, n$ the i -th term of the GCD approximation has the following form:

$$\begin{aligned} \left(DE_r(\omega^k, \varphi^k, \Lambda) \right)_i &= \frac{1}{2\mu_0} \sum_{\ell=i, i-1} \sum_{j=1}^K p_j \left(\frac{\partial \varphi^k}{\partial \nu_e} \right)^2 (x_l(s_j)) (Z_\ell^k \cdot \nu_e)(x_l(s_j)) L_l(s_j) \\ &+ \sigma \left(\frac{(z_i - z_{i-1})}{\|z_i - z_{i-1}\|} - \frac{(z_{i+1} - z_i)}{\|z_{i+1} - z_i\|} \right) \cdot \hat{Z}_i \\ &+ r \sum_{\ell=i, i-1} \sum_{j=1}^K p_j (Z_\ell^k \cdot \nu_e)(x_l(s_j)) \\ &\times \left(\sum_{\ell=i, i-1} \sum_{j=1}^K p_j \dot{x}_i^2(s_j) x_i^1(s_j) L_i(s_j) - S_0 \right) \end{aligned} \tag{58}$$

The first term is a numerical approximation of the first term of (57). This means that we make two approximations, namely the interpolation of the boundary and the numerical estimation of $\nabla \varphi^k \cdot \nu_e$. The term

$$\left(\frac{(z_i - z_{i-1})}{\|z_i - z_{i-1}\|} - \frac{(z_{i+1} - z_i)}{\|z_{i+1} - z_i\|} \right) \cdot \hat{Z}_i \tag{59}$$

is obtained by derivation of the perimeter of ω^k .

Having defined $\bar{S}(x)$ as the vector tangent to Γ^k at x , we introduce

$$\bar{S}_{i+1}^- = \lim_{\substack{z \rightarrow z_{i+1} \\ z \in (z_i, z_{i+1})}} \bar{S}(x) \tag{60}$$

and

$$\bar{S}_i^+ = \lim_{\substack{z \rightarrow z_i \\ z \in (z_i, z_{i+1})}} \bar{S}(x) \tag{61}$$

Hence (Sokolowski and Zolesio, 1992):

$$\frac{d}{dt} \left(\int_{\Gamma^k} d\Gamma \right) \Big|_{t=0} = \int_{\Gamma^k} \mathcal{H} Z_i \cdot \nu \, d\Gamma + \sum_{j=1}^n \hat{Z}_i \cdot (\bar{S}_j^- - \bar{S}_j^+) \tag{62}$$

Since \mathcal{H} is equal to zero for all l_i , we have (58).

This approach is used in (Novruzi and Roche, 1995; Pierre and Roche, 1991; 1993) for direct simulation in electromagnetic shaping metals.

Remark 10. The numerical computation of $(DE_r(\omega^k, \varphi^k, \Lambda))_i$ after solution the linear system (46) requires $2 \times K \times K \times O(n)$ flops for each i . Then the computation of the gradient after computation of φ^k demands $O(n^2)$ operations. This implies that the algorithm to compute the GCD approximation requires $(n^3/6) + O(n^2)$ floating-point operations. Clearly, this shows that the complexity of the algorithm is dominated by the solution of the linear system(46), more precisely the factorization step of the matrix A .

3.4. Gradient of the Discrete Cost Function

To compute the discrete gradient (GD, “Gradient Discret” in French) of the discrete cost function approximation, we consider first a discrete approximation of the penalized energy (33) and then we shall seek differences when we perturb $x_i(s)$ into $x_i(s) + \xi Z_\eta(s)$. We denote by D_η this derivative.

The discrete version of the penalized cost function is given by the following formula:

$$\begin{aligned} \bar{E}_r(w^k, \varphi^k) &= \frac{1}{2\mu_0} \sum_{i=1}^n \sum_{j=1}^K \left\{ p_j u^k(x_i(s_j)) \frac{\partial \bar{\varphi}^k(x_i(s_j))}{\partial \nu_e(x_i(s_j))} L_i(s_j) \right\} \\ &\quad + \sum_{i=1}^n \sum_{j=1}^K p_j \sigma L_i(s_j) \\ &\quad + \frac{r}{2} \left\{ \left(\sum_{i=1}^n \sum_{j=1}^K p_j \dot{x}_i^2(s_j) x_i^1(s_j) L_i(s_j) \right) - S \right\}^2 \\ &\quad + \int_{\text{supp}(j_0(y))} u(y) j_0(y) \, dy \end{aligned} \tag{63}$$

where the coefficients p_m appearing in the formula are in fact the weights associated with the interior Gauss-Legendre integration points $x_i(s_m)$, $i = 1, \dots, n$, $m = 1, \dots, K$.

Set

$$\frac{\partial \bar{\varphi}^k}{\partial \nu_e}(x_i(s_l)) = \frac{\partial \bar{u}^k}{\partial \nu_e}(x_i(s_l)) + \frac{\partial \bar{v}^k}{\partial \nu_e}(x_i(s_l)) \tag{64}$$

and

$$\frac{\partial \bar{v}^k}{\partial \nu_e}(x_i(s_l)) = \frac{-1}{2\pi} \sum_{\substack{j=1 \\ j \neq i}}^n q_j \sum_{m=1}^K p_m \frac{\partial \ln}{\partial \nu_e} |x_i(s_l) - x_j(s_m)| L_j(s_m) + \frac{1}{2} q_i \quad (65)$$

The coefficients q_j are the solutions to the linear system (46).

Formally, we can compute the following derivative:

$$\begin{aligned} D_\eta(\bar{E}_r(w^k, \varphi^k)) &= \frac{-1}{2\mu_0} \sum_{i=1}^n \sum_{m=1}^K p_m \left\{ D_\eta(u^k(x_i(s_m))) \frac{\partial \bar{\varphi}^k}{\partial \nu_e}(x_i(s_m)) L_i(s_m) \right. \\ &\quad + u^k(x_i(s_m)) D_\eta\left(\frac{\partial \bar{\varphi}^k}{\partial \nu_e}\right)(x_i(s_m)) L_i(s_m) \\ &\quad \left. + u^k(x_i(s_m)) \frac{\partial \bar{\varphi}^k}{\partial \nu_e}(x_i(s_m)) D_\eta(L_i(s_m)) \right\} \\ &\quad + \sum_{i=1}^n \sum_{m=1}^K p_m \sigma D_\eta(L_i(s_m)) \\ &\quad + r \left\{ \sum_{i=1}^n \sum_{m=1}^K p_m \left[D_\eta(\hat{x}_i^2(s_m) x_i^1(s_m)) L_i(s_m) \right. \right. \\ &\quad \left. \left. + \hat{x}_i^2(s_m) x_i^1(s_m) D_\eta(L_i(s_m)) \right] \right. \\ &\quad \left. \times \left[\left(\sum_{j=1}^n \sum_{l=1}^K p_l \hat{x}_j^2(s_l) x_j^1(s_l) \right) - S \right] \right\} \quad (66) \end{aligned}$$

where:

- i) $D_\eta(u^k(x_i(s_m))) = \nabla u^k(x_i(s_m)) Z_\eta(x_i(s_m))$
- ii) $D_\eta(L_i(s_m)) = L_i^{-1}(s_m) \dot{x}_i^t(s_m) \cdot D_\eta(\dot{x}_i(s_m))$
- iii) $D_\eta(\hat{x}_i^2(s_m) x_i^1(s_m)) = D_\eta(\hat{x}_i^2(s_m)) x_i^1(s_m) + \hat{x}_i^2(s_m) D_\eta(x_i^2(s_m))$

$$\begin{aligned}
 \text{iv) } D_\eta \left(\frac{\partial \bar{v}^k}{\partial \nu_e} (x_i(s_\ell)) \right) &= \frac{-1}{2\pi} \sum_{\substack{j=1 \\ j \neq i}}^n D_\eta(q_j) \sum_{m=1}^K p_m \frac{\partial \ln}{\partial \nu_e} |x_i(s_\ell) - x_j(s_m)| L_j(s_m) \\
 &\quad + \frac{1}{2} D_\eta(q_i) \\
 &\quad - \frac{1}{2\pi} \sum_{\substack{j=1 \\ j \neq i}}^n (q_j) \sum_{m=1}^K p_m D_\eta \left(\frac{\partial \ln}{\partial \nu_e} |x_i(s_\ell) - x_j(s_m)| \right) \\
 &\quad \quad \times L_j(s_m) \\
 &\quad - \frac{1}{2\pi} \sum_{\substack{j=1 \\ j \neq i}}^n (q_j) \sum_{m=1}^K p_m \frac{\partial \ln}{\partial \nu_e} |x_i(s_\ell) - x_j(s_m)| \\
 &\quad \quad \times D_\eta(L_j(s_m)) \tag{67}
 \end{aligned}$$

The $D_\eta(q_j)$'s are the shape derivatives of q_j , $j = 1, \dots, n$. The vector $D_\eta(\bar{q})$ is then the solution to the following linear system:

$$AD_\eta(\bar{q}) = D_\eta(b) - D_\eta(A)\bar{q} \tag{68}$$

where

$$D_\eta(\bar{q}) = (D_\eta(q_j))_{j=1, \dots, n}^t \tag{69}$$

$$D_\eta(b) = (D_\eta(b_j))_{j=1, \dots, n}^t \tag{70}$$

and

$$D_\eta(A) = (D_\eta(a_{ij}))_{i,j=1, \dots, n} \tag{71}$$

Here A, b and \bar{q} are given by (46)–(50), (53) and (51), respectively.

To compute the matrix coefficients $D_\eta(a_{ij})$, $i, j = 1, \dots, n$, we make use of the expressions

$$a_{ij} = \frac{1}{4\pi} \left(\sum_{m_1=1}^K \sum_{m_2=1}^K w_{m_1} w_{m_2} \ln |x_i(s_{m_1}) - x_j(s_{m_2})| L_i L_j \right) \tag{72}$$

if $i \neq j$, and

$$a_{ii} = \frac{1}{4\pi} (\ln L_i^2 - 3) L_i^2 \tag{73}$$

Accordingly,

$$\begin{aligned}
 D_\eta(a_{ij}) &= \frac{1}{4\pi} \left\{ \sum_{m_1=1}^K \sum_{m_2=1}^K w_{m_1} w_{m_2} \left[D_\eta(\ln |x_i(s_{m_1}) - x_j(s_{m_2})|) L_i L_j \right. \right. \\
 &\quad \left. \left. + \ln |x_i(s_{m_1}) - x_j(s_{m_2})| D_\eta(L_i) L_j \right. \right. \\
 &\quad \left. \left. + \ln |x_i(s_{m_1}) - x_j(s_{m_2})| L_i D_\eta(L_j) \right] \right\} \text{ if } i \neq j \tag{74}
 \end{aligned}$$

and

$$D_\eta(a_{ii}) = \frac{1}{2\pi} (L_i D_\eta(L_i)) (\ln L_i^2 - 2) \tag{75}$$

Since

$$b_i = - \sum_{k=1}^K p_k u(x_i(s_k)) L_i, \quad i = 1, \dots, n \text{ and } b_{n+1} = 0 \tag{76}$$

we have

$$D_\eta(b_i) = - \sum_{m=1}^K p_m \left\{ D_\eta(u(x_i(s_m))) L_i + u(x_i(s_m)) D_\eta(L_i) \right\} \tag{77}$$

In conclusion, we obtain the following result:

Theorem 1. *Let Ω be a domain with piecewise linear boundary Γ . If $\bar{E}_r(w^k, \varphi^k)$ is given by (63), then the shape derivative $D_\eta(\bar{E}_r(w^k, \varphi^k))$ is given by*

$$\begin{aligned} D_\eta(\bar{E}_r(w^k, \varphi^k)) &= \frac{-1}{2\mu_0} \sum_{i=1}^n \sum_{m=1}^K p_m \left\{ D_\eta(u^k(x_i(s_m))) \frac{\partial \bar{\varphi}^k}{\partial \nu_e}(x_i(s_m)) L_i(s_m) \right. \\ &\quad + u^k(x_i(s_m)) D_\eta\left(\frac{\partial \bar{\varphi}^k}{\partial \nu_e}\right)(x_i(s_m)) L_i(s_m) \\ &\quad \left. + u^k(x_i(s_m)) \frac{\partial \bar{\varphi}^k}{\partial \nu_e}(x_i(s_m)) D_\eta(L_i(s_m)) \right\} \\ &\quad + \sum_{i=1}^n \sum_{m=1}^K p_m \sigma D_\eta(L_i(s_m)) \\ &\quad + r \left\{ \sum_{i=1}^n \sum_{m=1}^K p_m \left[D_\eta(\dot{x}_i^2(s_m) x_i^1(s_m)) L_i(s_m) \right. \right. \\ &\quad \left. \left. + \dot{x}_i^2(s_m) x_i^1(s_m) D_\eta(L_i(s_m)) \right] \right. \\ &\quad \left. \times \left[\left(\sum_{j=1}^n \sum_{l=1}^K p_l \dot{x}_j^2(s_l) x_j^1(s_l) \right) - S \right] \right\} \tag{78} \end{aligned}$$

Remark 11. To compute the GD approximation, we have to solve the linear system (68) for $\eta = 1, \dots, n$. As the matrix A was factorized to solve the linear system (46), the solution to the linear system (68) requires n^2 operations for each η , so that this step adds $n^3 + O(n^2)$ flops to the number of operations required to compute the GD approximation. The number of floating point operations needed to compute the GD approximation is $n^3 + (n^3/6) + O(n^2)$.

4. Numerical Algorithm

The numerical method consists in constructing a sequence of Γ^k piecewise linear Jordan curves given by (30). At each iteration the vector $\bar{\xi}_{k+1} \in \mathbb{R}^n$ is computed by a Quasi-Newton optimization procedure such that:

$$E_r(\bar{\xi}_{k+1}) \leq E_r(\bar{\xi}_k) \tag{79}$$

We propose the following scheme to evaluate the unknown optimal shape, as a local minimum of (1):

Data. Γ^0 , r^0 , the perturbation vector field Z and \bar{j}_0 given.

For $r = r^k$ solve the unconstrained optimization problem:

$$(P_r) \quad \min \left\{ E_r(\bar{\xi}), \bar{\xi} \in \mathbb{R}^n \right\} \tag{80}$$

for $k = 0, 1, \dots$ until a convergence test is satisfied:

Step 0. Set $k = 0$, $H_k =$ the identity matrix.

Step 1. Compute the gradient of E_r .

a) Solve the integral equations (42) and (43).

Here we have two possibilities:

b1) Compute the GCD of E_r , or

b2) Compute the GD of the approximation of E_r .

Step 2. Compute the descent direction using a BFGS approximation of the Hessian of E_r . For $g_k = DE_r(\bar{\xi}_k) - DE_r(\bar{\xi}_{k-1})$ and $\delta_k = \bar{\xi}_k - \bar{\xi}_{k-1}$ compute H_{k+1} as

$$H_{k+1} = H_k + \left[\frac{1 + g_k^t H_k \delta_k}{\delta_k^t g_k} \right] \frac{\delta_k \delta_k^t}{\delta_k^t g_k} - \frac{\delta_k^t g_k H_k + H_k g_k \delta_k^t}{\delta_k^t g_k} \tag{81}$$

Step 3. Compute

$$\bar{\xi}_{k+1} = -\rho_k (H_k DE_r(\bar{\xi}_k)) \tag{82}$$

where ρ_k is found by the Wolfe line-search procedure.

Step 4. Update the boundary Γ^k to obtain Γ^{k+1}

$$\Gamma^{k+1} = \left(I + \sum_{l=1}^m \{ \bar{\xi}_{k+1} \}_l Z_l \right) (\Gamma^k) \tag{83}$$

Set $k = k + 1$. Return to Step 1.

Remark 12. The first value r^0 of the penalty parameter r must be chosen so that the penalty term be of the same order as the gradient of E . Otherwise, numerical instabilities may occur. After solving the unconstrained problem E_{r^0} , only two or three steps in the evolution of the parameter r are needed to guarantee the convergence, e.g. $r = 10, 100, 1000$. The number of steps k to solve the unconstrained problem (P_r) depends on the test of convergence and r . For the first r -iteration we terminate the iteration when $k = 20$, but for the last r -iteration we stop when the gradient norm stops decreasing.

Remark 13. In (Dennis and Schnabel, 1983) the authors remark that to get H_{k+1} from H_k requires $O(n^2)$ operations. Accordingly, the GCD method requires $(n^3/6) + O(n^2)$ flops at each iteration and the GD method requires $n^3 + (n^3/6) + O(n^2)$ flops at each iteration. This implies that an iteration of the GD method requires n^3 more flops than one GCD iteration.

We also remark that the finite-difference approximation of the gradient, which is classical in engineering, requires $O(n^4)$ operations because of the n numerical resolutions of the exterior problem at each iteration.

5. Numerical Examples

In order to illustrate the differences between the two methods, we consider two examples described in (Pierre and Roche, 1991). We estimate the differences in the L^2 -norm between the GD of the penalized cost function and the GCD of the penalized cost function at each iteration when we use the algorithm presented in the previous section. In each example, the surface tension and the surface S_0 of the liquid are given in addition to the distribution of the current j_0 which is of the form

$$j_0 = \left(\sum_{p=1}^m \alpha_p \delta_{x_p} \right) I \quad (84)$$

where I is a given intensity of the current, δ_{x_p} , $p = 1, \dots, m$ are the Dirac masses at the points x_p in the plane, and α_p are adimensional coefficients which are directly indicated on the figures.

In the first example, we consider four Dirac masses and a surface of S equal to π . In Table 1, the first column gives the number of evaluations of the gradient, while the second column gives the L^2 -norm of the discretized continuous gradient and the L^2 -norm of the difference between the GCD and GD when we run the GCD algorithm. In Table 2, we observe the evolution of the L^2 -norm of the GD and the difference between the GCD and GD when we use the GD algorithm. Figures 1 and 2 show the corresponding plots.

In the second example, we consider twelve Dirac masses for $\sigma = 0.5$ and $S = 4$. In Table 3, we observe the evolution of the GCD and the error with respect to the GD. In Table 4, we show the evolution of the GD and the error with respect to the GCD. The respective graphs are displayed in Figs. 3 and 4.

Table 1. Example 1, $n = 64$, $\sigma = 0.005$, GCD gradient.

| iter. | $\ \text{GCD}\ _{L^2(\Gamma)}$ | $\ \text{GCD} - \text{GD}\ _{L^2(\Gamma)}$ |
|-------|--------------------------------|--|
| 10 | 0.128e-02 | 0.363e-03 |
| 30 | 0.871e-03 | 0.353e-03 |
| 50 | 0.334e-03 | 0.272e-03 |
| 100 | 0.180e-03 | 0.200e-03 |
| 146 | 0.133e-03 | 0.206e-03 |

Table 2. Example 1, $n = 64$, $\sigma = 0.005$, GD gradient.

| iter. | $\ \text{GD}\ _{L^2(\Gamma)}$ | $\ \text{GCD} - \text{GD}\ _{L^2(\Gamma)}$ |
|-------|-------------------------------|--|
| 10 | 0.154e-02 | 0.364e-03 |
| 30 | 0.140e-03 | 0.254e-03 |
| 50 | 0.981e-04 | 0.210e-03 |
| 70 | 0.869e-04 | 0.198e-03 |
| 100 | 0.787e-04 | 0.198e-03 |
| 181 | 0.742e-04 | 0.206e-03 |

Table 3. Example 2, $n = 64$, $\sigma = 0.5$, GCD.

| iter. | $\ \text{GCD}\ _{L^2(\Gamma)}$ | $\ \text{GCD} - \text{GD}\ _{L^2(\Gamma)}$ |
|-------|--------------------------------|--|
| 10 | 0.285 | 0.777e-02 |
| 30 | 0.136 | 0.513e-02 |
| 50 | 0.671e-01 | 0.443e-02 |
| 70 | 0.312e-01 | 0.414e-02 |
| 100 | 0.416e-02 | 0.340e-03 |
| 200 | 0.169e-03 | 0.199e-02 |
| 321 | 0.156e-05 | 0.195e-02 |

Table 4. Example 2, $n = 64$, $\sigma = 0.5$, GD.

| iter. | $\ \text{GD}\ _{L^2(\Gamma)}$ | $\ \text{GCD} - \text{GD}\ _{L^2(\Gamma)}$ |
|-------|-------------------------------|--|
| 10 | 0.288 | 0.845e-02 |
| 30 | 0.753e-01 | 0.635e-02 |
| 50 | 0.361e-01 | 0.578e-02 |
| 70 | 0.148e-02 | 0.359e-02 |
| 100 | 0.541e-03 | 0.265e-02 |
| 200 | 0.630e-04 | 0.219e-02 |
| 300 | 0.656e-05 | 0.219e-02 |
| 415 | 0.853e-06 | 0.219e-02 |

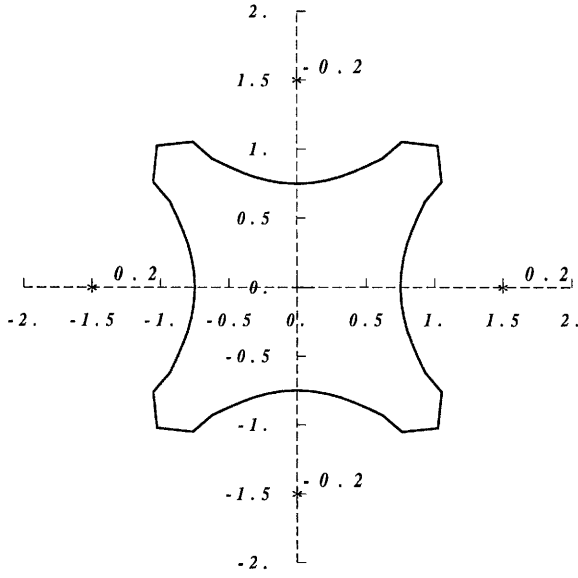


Fig. 1. Results of Example 1 obtained using the GCD.

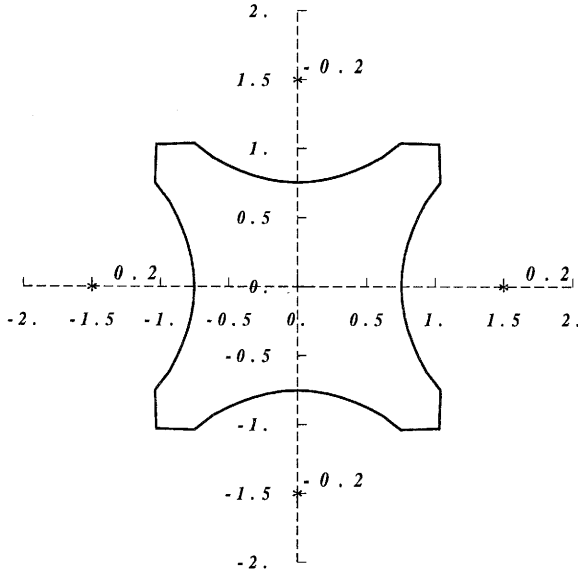


Fig. 2. Results of Example 1 obtained using the GD.

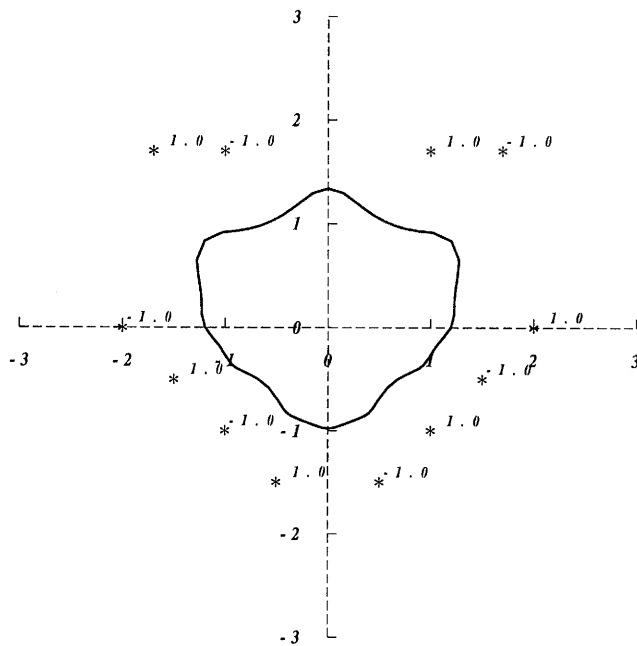


Fig. 3. Results of Example 2 obtained after 321 iterations using the GCD.

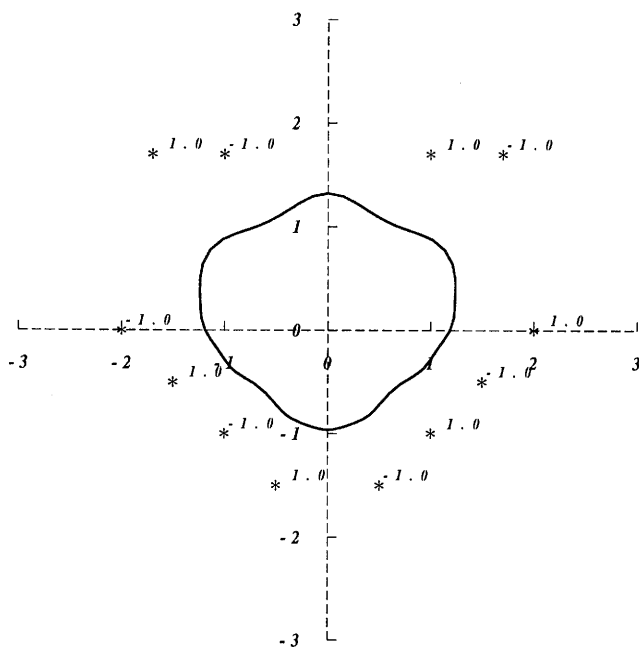


Fig. 4. Results of Example 2 obtained after 415 iterations using the GD.

In Tables 1–4 we observe that the method using the GD has a rate of convergence greater than that of methods using the GCD. The two examples presented show that the GD allows us to compute a better approximation of the solution of the discretized Euler condition. This is a natural conclusion, since the GCD is only an approximation of the GD. But the local optimal shapes obtained by the two methods are similar and the differences do not justify the extra floating-point operations required to compute the GD.

In conclusion, we think that the GCD method to compute an approximation of the gradient is more efficient because it gives accurate results at a low floating-point operation cost.

References

- Adams R., (1989): *Sobolev Spaces*. — San Diego: Academic Press.
- Brancher J.P., Etay J. and Sero-Guillaume O. (1983): *Formage d'une lame*. — J. Mécanique Théorique et Appliquée, Vol.2, No.6, pp.976–989.
- Brancher J.P., Sero-Guillaume O. (1983): *Sur l'équilibre des liquides magnétiques, applications à la magnétostatique*. — J. Mécanique Théorique et Appliquée, Vol.2, No.2, pp.265–283.
- Chenais D. (1992): *Discrete gradient and discretized continuum gradient in shape optimization of shells*. — Preprint, No.313, Université de Nice.
- Costabel M. and Stephan E.P. (1985): *Boundary integral equations for mixed boundary value problems in polygonal domains and Galerkin approximations*, In: *Mathematical Models and Methods in Mechanics* (Fiszdon W. and Wilmanski K., Eds.). — Warsaw: PWN.
- Coulaud O. and Henrot A. (1994): *Numerical approximation of a free boundary problem arising in electromagnetic shape*. — SIAM J. Numer. Anal., Vol.31, No.4, pp.1109–1127.
- Dennis J.E. and Schnabel R.B. (1983): *Numerical Methods for Unconstrained Optimization and Nonlinear Equations*. — New Jersey, Englewood Cliffs: Prentice-Hall.
- Etay J. (1982): *Le formage électromagnétique des métaux liquides. Aspects expérimentaux et théoriques*. — Thèse Docteur-Ingénieur, U.S.M.G., I.N.P.G. Grenoble, France.
- Fiacco A.V. and McCormick G.P. (1968): *Nonlinear Programming. Sequential Unconstrained Minimization Techniques*. — New York: J. Wiley.
- Fletcher R. (1987): *Practical Methods of Optimization*. — Chichester: J. Wiley.
- Gagnoud A., Etay J., Garnier M. (1986): *Le problème de frontière libre en lévitation électromagnétique*. — J. Mécanique Théorique et Appliquée, Vol.5, No.6, pp.911–925.
- Grisvard P. (1985): *Elliptic Problems in Nonsmooth Domains*. — Boston: Pitman Adv. Publ. Program.
- Golub G.H., Van Loan C.F., (1983): *Matrix Computation*. — Baltimore: The Johns Hopkins University Press.
- Henrot A. and Pierre M. (1989): *Un problème inverse en formage de métaux liquides*. — *M.²A.N.*, Vol.23, No.1, pp.155–177.

- Kress R. (1982): *Linear Integral Equations*. — Appl. Math. Sciences, Vol.82, Berlin: Springer-Verlag.
- Lods V. (1992): *Gradient discret et gradient continu discrétisé en contrôle optimal à paramètres distribués*. — Thèse de l'Université de Nice.
- Masmoudi M. (1987): *Outils pour la conception optimale de formes*. — Thèse de l'Université de Nice.
- Mestel A.J. (1982): *Magnetic levitation of liquid metals*. — J. Fluid Mech., Vol.117, pp.27–43.
- Minoux M. (1983): *Programmation Mathématique, Théorie et algorithmes, tome 1*. — Paris: Dunod.
- Nedelec J.C. (1977): *Approximation des équations intégrales en mécanique et en physique*. — Rapport interne, Ecole Polytechnique, Centre de Mathématiques Appliquées. Palaiseau, France.
- Novruzi A. and Roche J.R. (1995): *Second order derivatives, Newton method, applications to shape optimization*. — Report INRIA No.2555, Paris, France.
- Pierre M. (1992): *Optimisation des formes*. — Cours D.E.A., Université de Nancy I.
- Pierre M. and Roche J.R. (1991): *Numerical computation of free boundaries in 2-d electromagnetic shaping*. — Eur. J. Mech. B/Fluids, Vol.10, No.5, pp.489–500.
- Pierre M. and Roche J.R. (1993): *Numerical simulation of tridimensional electromagnetic shaping of liquid metals*. — Numer. Math., Vol.65, No.2, pp.203–217.
- Shercliff J.A. (1981): *Magnetic shaping of molten metal columns*. — Proc. Royal. Soc., Vol.375, No.1763, pp.455–473.
- Sneyd A.D. and Moffat H.K. (1982): *Fluid dynamical aspects of the levitation melting process*. — J. Fluid Mech., Vol.117, pp.45–70.
- Sero-Guillaume O. (1983): *Sur l'équilibre des ferrofluides et des métaux liquides*. — Thèse, Inst. Polytechnique de Lorraine, Nancy, France.
- Simon J. (1980): *Differentiation with respect to the domain in boundary value problems*. — Num. Funct. Anal. Optim., Vol.2, pp.649–687.
- Sokolowski J. and Zolesio J.P. (1992): *Introduction to Shape Optimization. Shape Sensitivity Analysis*. — Computational Mathematics, Vol.16, New York: Springer-Verlag.

Received: 18 September, 1996